Role of metal contacts in the mechanical properties of molecular nanojunctions: Comparative *ab initio* study of Au/1,8-octanedithiol and Au/4,4-bipyridine

P. Vélez,[1] S. A. Dassie,[1,2] and E. P. M. Leiva[1,*]

[1]*Departamento de Matemática y Física–INFIQC, Facultad de Ciencias Químicas, Universidad Nacional de Córdoba, Ciudad Universitaria, X5000HUA Córdoba, Argentina*

[2]*Departamento de Fisicoquímica–INFIQC, Facultad de Ciencias Químicas, Universidad Nacional de Córdoba, Ciudad Universitaria, X5000HUA Córdoba, Argentina*

(Received 19 March 2010; published 28 June 2010)

A comparative study of the mechanical properties of Au/4,4′-bipyridine (4,4′ BPD) and Au/1,8-octanedithiol (1,8 ODT) molecular nanojunctions is developed using different metal wires and small clusters to represent the metal contact. Rupture of the junction at different bonds is analyzed. While in the case of 1,8 ODT, rupture at Au-Au bonds is always found; in the case of 4,4′ BPD, rupture of a N-Au bond also appears as possible. Comparison of rupture forces, maximum elongations and force constants with the experimental values lead to the conclusion that the most common geometrical arrangement in scanning tunneling microscopy break junctions should be that where the number of Au atoms is of the order of 4. Activation energies for the rupture of these structures are calculated at sample elongations.

DOI: 10.1103/PhysRevB.81.235435 PACS number(s): 73.63.Rt, 73.63.Nm, 73.63.Bd, 73.21.Hb

I. INTRODUCTION

Early studies in the literature concerning the conductance of nanocontacts based on an atomistic picture of the system were accompanied by the first studies on the plastic deformation of these structures. A pioneering work in this area was performed by Agrait and co-workers.[1] These authors combined atomic force microscopy (AFM) and scanning tunneling microscopy (STM) to study the mechanical nature of a nanoneck formed between a tip and a substrate of the same metal (Au). Force and conductance were measured simultaneously during the formation and rupture of an atomic-sized contact at room temperature. These experiments confirmed that the variation of conductance in steps, when the STM tip is moved away perpendicularly to the substrate, is due to the alternation of elastic stages that take place in the deformation process. During stretching, the slopes of the force-distance curves were found more or less constant until the subsequent relaxation induced by atomic rearrangements. Furthermore, the conductance values remained constant during the elastic stages of force observed after an abrupt change in its value when the forces relax. The conductance observed in the last step was constant (0.98 ± 0.07 G_0) and the breaking force was 1.5 ± 0.2 nN. This value is in agreement with other experimental results[2,3] and theoretical calculations.[2,4–9] In a later work, Rubio-Bollinger and co-workers[2] found that monatomic chains of Au are five times harder than their bulk material. The average value of the spring force for an average chain length was 8 N/m.

Another interesting aspect of the mechanics of these systems, confirmed experimentally[1–3,10–12] and theoretically,[4,8,13–15] is that monatomic Au chains contain on the average 4 Au atoms in the moment right before its breakup. This feature denotes the singular drawability of Au upon mechanical stretching and also denotes that the elongation of the system is limited by the maximum number of Au atoms that may build the nanowire.

In recent years, numerous research groups have focused on the study of electrical and mechanical properties of molecular nanojunctions. Typically, the generation of these nanostructures is carried out by the impact of an STM tip against a metal surface and subsequent retraction or via the application of the mechanically controlled break junction (MCBJ) method. A large number of experimental[16–29] and theoretical[30–39] studies of the conductance of various molecular nanojunctions can be found in the literature, particularly those where the molecule has sulfur and nitrogen atoms at its ends, thus, ensuring its binding to the Au electrodes. A review of recent advances in the understanding of properties of nanojunctions can be found in Ref. 40. However, at present, there are relatively few mechanistic studies of such systems. Much knowledge in this area is due to the efforts of Tao´s group, who from the combined measurement of force and conductance[18–22] has been able to clarify some important mechanical aspects of these molecular nanojunctions. In Ref. 21, these authors measured the conductance and the maximum force required to break 1,8-octanedithiol and 4,4′-bipyridine molecular nanojunctions, covalently linked to two Au electrodes. The force histograms showed pronounced peaks with a characteristic force quantum 0.80 ± 0.2 nN when the nanojunction is formed using a 4,4′-bipyridine molecule and 1.50 ± 0.2 nN in the case of 1,8-octanedithiol nanojunction. In the first case, the maximum force encountered was assigned to the Au-N bond breaking and the second, to the Au-Au bond breaking, which is expected due to strong covalent interaction between atoms Au and S. The multiple peaks in the force histograms were attributed to the rupture force of multiple molecular nanojunctions. The distance that a molecular nanojunction can be elongated before breaking was determined from individual curves of conductance and force. Histograms of the maximum elongation (see Supporting Information of Ref. 21) have a somewhat scattered distribution, so the authors reported an average value equal to 3 Å for 4,4′-bipyridine and 3.5 Å for 1,8-octanedithiol nanojunctions. In these experiments, the spring force was calculated as the average slope of the force curves referred to last elongation stage.

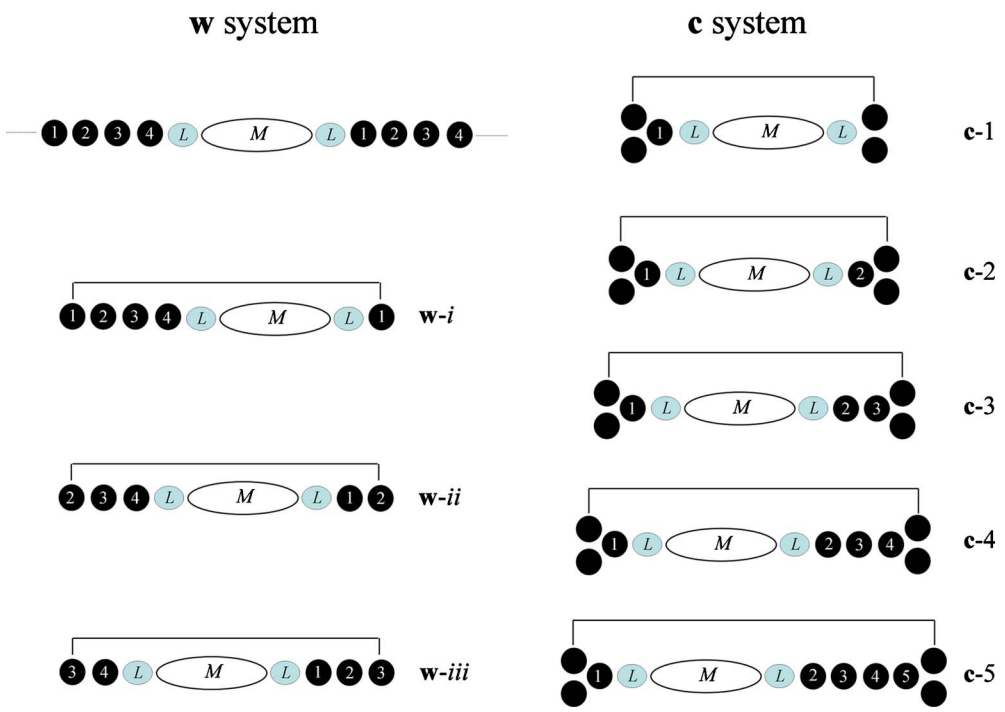

FIG. 1. (Color online) Schematic representation of the supercell used for the study of 4,4′ BPD and 1,8 ODT molecular nanojunctions. The ellipse marked with *M* denotes the body of the molecule, and the circle *L* denotes the link atom, (S or N in the present case). The **w** system considers a chain of 4 atoms attached to a 4,4′-bipyridine or 1,8-octanedithiol molecule. Different elongation types of the unit cell are considered in order to attempt the rupture of the wire at three different bonds: **w**-*i* [attempt to break at the $S_2(N_2)$-Au_1 link], **w**-*ii* (attempt to break the Au_1-Au_2 link) and **w**-*iii* (attempt to break the Au_2-Au_3 link).

The distribution of these values (see Supporting Information of Ref. 21) is sharper than that of that of the elongations, and while the authors preferred to report average values it can be seen that the most probable spring force constant are 3.4 N/m for 4,4′-bipyridine and 5 N/m for the 1,8-octanedithiol nanojunctions, respectively. The valuable amount of information reported in this work[21] motivated us to conduct the studies and analysis presented here.

Concerning the theoretical study of the mechanical properties of molecular nanojunctions, we can highlight the work of Marx and co-workers.[41,42] Using first principles calculations,[41] these authors elongated mechanically a junction made of a methanethiolate molecule bound to a Au cluster of 5 atoms, drawing from it a monatomic Au chain. They obtained a final rupture of the system at a Au-Au bond, with a rupture force very close to the experimental value.[18–22] These authors also made a pioneering Car-Parrinello molecular dynamics simulation[42] stretching an ethanethiolate molecule bound to a defective Au surface, obtained similar results and conclusions.

Most theoretical studies on the molecular nanojunction 4,4′-bipyridine/Au have been oriented toward the calculation of the conductance of these systems.[33–39] On the other hand, there are currently few contributions concerning studies of the mechanical properties of this nanojunction.[7,33] Something similar can be stated on other equivalent Au-N systems, as it is the case of the nanojunction involving the pyrazine molecule[7,43] and ortho substituted pyrazines molecules.[43,44]

In this paper, we will study comparatively from first principles calculations, the 1,8-octanedithiol and 4,4′-bipyridine molecular nanojunctions involving Au electrodes. The analysis will focus on the stability of such systems when subjected to mechanical stretching. The calculation are oriented to predict properties obtained experimentally[21] such as the rupture force, the spring force and the maximum elongation of these molecular nanojunctions.

II. CALCULATION MODEL AND COMPUTATIONAL DETAILS

Figure 1 shows the supercells of the two models used for calculations for the 1,8-octanedithiolate (1,8 ODT) and the 4,4′-bipyridine (4,4′ BPD) molecular nanojunctions. In this figure, the ellipse marked with *M* denotes the body of the molecule, and the circle *L* denotes the link atom, (S or N in the present case). Both systems are placed along the *z* axis with periodic boundary conditions. The extension of the unit cell is depicted for all structures considered. The **w** system represents a simplified calculation model, where the molecule is linked to a monatomic Au chain of 4 atoms. To take into account all possible rupture of the **w** system, we have considered three different options to stretch the unit cell. Thus, depending on the choice, the atoms Au_1, Au_2, or Au_3 on the left were kept fixed and the length of unit cell was changed, thus moving its image to the right in the case of the **w**-*i*, **w**-*ii*, or **w**-*iii* systems, respectively. After each stretching of the unit cell, the energy of the system was minimized using the conjugated gradient (CG) method. The purpose of this procedure was to try to induce rupture at the *L*-Au_1, Au_1-Au_2, and Au_2-Au_3 bonds, respectively, which represent

the plausible possibilities in the present case.

The **c** system, based on a cluster of 4 atoms, incorporates gradually Au atoms at the right end of the nanojunction. In this system, the Au atoms that remain fixed during relaxation form a triangular base with distances corresponding to those of first neighbors of the gold fcc structure (2.88 Å).

In the experimental system, the molecular nanojunctions are created from repeated movements of an STM tip colliding with the Au surface in a solution containing 4,4′ BPD[21,23] or 1,8 ODT[18–24] molecules. This process forms a monatomic Au chain that finally breaks, resulting in the incorporation of the molecule between two Au electrodes. A situation where the molecule is attached to one of the electrodes through a monatomic chain of Au atoms is, therefore, very likely. The formation of Au chains made of up to 4 atoms has been experimentally observed[1–3,10–12] and verified by theoretical and computational calculations.[4,8,13–15] Organic molecules with terminal sulfur atoms bind very strongly to Au electrodes and from a theoretical point of view there is evidence that these molecules may pull Au atoms from the surface in a mechanical stretching procedure.[41,42] The Au-N interaction, like the present in 4,4′ BPD and pyrazine nanojunctions is weaker, with a lower degree of covalency. However, because of the way in which these nanojunctions are generated, where Au wires may be pre-existent, it is necessary to consider that these molecules may attach to the Au electrode through a monatomic chain.

The first-principles calculations within the framework of density functional theory (DFT) were performed with the SIESTA code.[45–49] The valence electrons were described with a set of double-z polarized bases. The number of k points in the z direction were increased to obtain convergence in the system energy better than 0.002 eV/atom, resulting a sample of $1\times1\times30$ k-points finally. The separation in the x-y plane between the neighboring molecular nanojunctions was 20 Å to ensure convergence in the system energy. The exchange and correlation effects were described using the generalized gradient approximation (GGA) in the functional Perdew-Burke-Ernzerhof.[24] The *energy shift* used to confine the electrons in the pseudoatomic orbitals was 0.005 eV. This value led to converged results for the present systems. For some sample structures of the molecular nanojunctions we performed calculations with and without spin polarization obtaining identical results.

To emulate the experimental mechanical stretching, we relaxed the atomic coordinates of the nanojunctions by the conjugate gradient technique, using a standard tolerance on the forces of 0.01 eV/Å. The length of the unit cell was increased as described above in steps of length $\Delta z=0.1$ Å, thus, beginning a new stage of system energy minimization. As the total system energy E is calculated at each minimization stage, this allows to evaluate the system force in the z direction of elongation according to $F_z=-\partial E(\Delta z)/\partial\Delta z$, which should be equivalent to the experimental stretching force. As we will see later, the behavior of F_z is in many cases (but not in all) elastic-like from zero to the maximum rupture force F_z^*. This allows the calculation of an average spring force k_z of the system from the linear approximation $F_z=k_z\Delta z$. In any case, the way in which we calculate k_z allows comparison with the spring force determined experimentally.[21] For all cases, the elongation of the system Δz is referred to the situation where $F_z\sim0$ and the energy of the system is also referred to this state $[E(\Delta z=0)=0]$.

TABLE I. Relevant bond distances d(i,j) and torsion angle θ_t for the equilibrium configuration of the 4,4′ BPD nanojunction of the **w** system. The structure shown below corresponds to the supercell of the equilibrium configuration.

d(1,2) (Å)	d(2,3) (Å)	d(3,4) (Å)	d(4,N_1) (Å)	d(N_2,1) (Å)	θ_t (°)
2.57	2.68	2.57	2.18	2.16	31.1

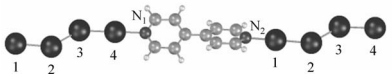

In the case of the calculation of activation energies, we used the double nudged elastic band (DNEB) method[50] associated with the minimization algorithm limited memory Broyden-Fletcher-Goldfarb-Shanno (L-BFGS)[51] to find the minimum energy path (MEP) between the configurations corresponding to linked and fragmented nanowires. On the average, the methodology DNEB/L-BFGS required only 30 iterations for convergence. The calculations to find the MEP were conducted with 12 images.

III. RESULTS AND DISCUSSION

A. w system

Tables I and II show structural information on the equilibrium configurations of 4,4′ BPD and 1,8 ODT molecular nanojunctions, respectively, for the **w** system. The N-Au equilibrium bond distances and the torsion angle θ_t between the pyridine rings to are in good agreement with theoretical values cited in literature.[38,52] The torsion angle value (31.1°) is slightly smaller than that of an isolated molecule of 4,4′ BPD as determined experimentally (37.2°).[53]

The S-Au equilibrium bond distance found for 1,8 ODT (2.31 Å) is equivalent to the S-Au distance of an organic molecule with a thiolate terminal group adsorbed on top of a Au atom on a (111) single crystal surface, as determined computationally.[54]

As described in Sec. II and shown in Fig. 1, in the case of the **w** system different attempts were made to break the junc-

TABLE II. Relevant bond distances d(i,j) for the equilibrium configuration of the 1,8 ODT nanojunction of the **w** system. The structure shown below corresponds to the supercell of the equilibrium configuration.

.

d(1,2) (Å)	d(2,3) (Å)	d(3,4) (Å)	d(4,S_1) (Å)	d(S_2,1) (Å)
2.64	2.64	2.64	2.31	2.31

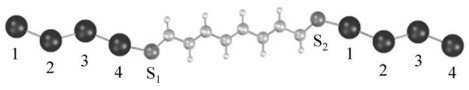

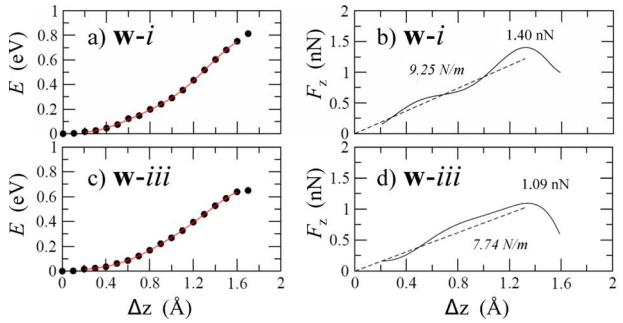

FIG. 2. (Color online) a) and c) System energy E as a function of elongation Δz for the **w**-*i* and **w**-*iii* systems respectively. 4,4′ BPD nanojunction. b) and d) z component of the force F_z (solid curve) as a function of elongation Δz and linear fit of F_z (dashed line) from zero to the maximum force value F_z^* for the **w**-*i* and **w**-*iii* systems, respectively. Values in normal font indicate the maximum rupture force F_z^* and values in italics indicate the force constants k_z (slopes of the dashed lines) of the different systems.

tion in different sites via elongation of the unit cell in different ways. In the case of 4,4′ BPD, stretching with the **w**-*i* and **w**-*ii* configurations lead to rupture at the N_2-Au_1 bond, while stretching with the **w**-*iii* configuration leads to rupture at the Au_2-Au_3 bond. The fact that the attempt to break the Au_1-Au_2 bond (**w**-*ii* system) concludes with a rupture at the N_2-Au_1 bond, denotes the particular stability of the Au-Au bond neighboring the nitrogen atom. Figure 2 shows the system energy and the force curve for the **w**-*i* and **w**-*iii* systems.

The maximum force found for rupture at the N_2-Au_1 bond [1.40 nN, Fig. 2(b)] is significantly higher than the corresponding maximum force found for rupture at the Au_2-Au_3 bond [1.09 nN, Fig. 2(d)]. A consistent result is found for the energy of the system [Figs. 2(a) and 2(c)], where it is found that the stretching procedure leading to rupture at the Au_2-Au_3 bond always leads to more stable configurations. Table III summarizes the structural information of the different configurations at the point of maximum force and mechanical information of the three stretching procedures performed with the **w** system for the 4,4′ BPD molecular nanojunction.

The previous results indicate that when the molecule is attached to a Au monatomic chain, this system should not break in the N-Au bond as suggested by the experimental results of Ref. 21, but rather at a Au-Au bond. Moreover, the agreement between the k_z and Δz^* values reported in Table III for the **w** system and the experiment values (k_z =3.4 N/m and Δz^*=3.0 Å) is not entirely satisfactory, especially in the case of Δz^*. In fact, a larger force constant and a shorter elongation indicate that the theoretical system proposed is stiffer that the actual structure of the junction. We will improve these points in the c system discussed below.

Similarly to the case of 4,4′ BPD, three different stretching types were also considered for the 1,8 ODT **w**-system, with the results given in Table IV. They lead in all cases to rupture at one of the Au-Au bonds. The **w**-*i* and **w**-*iii* systems were found to break at the Au_2-Au_3 bond yielding equivalent cases, while the **w**-*ii* system broke at the Au_1-Au_2 bond. The former presented rupture forces values very close

TABLE III. Relevant bond distances d(i,j) and torsion angles θ_t at the rupture configurations of the **w** system of the 4,4′ BPD nanojunction. F_z^*, k_z and Δz^* denote the rupture force, force constant and maximum elongation respectively and **w**-*i*, **w**-*ii*, and **w**-*iii* indicate the rupture procedure according to Fig. 1. The bond distances where rupture occurs are highlighted in bold. The rupture configurations of the three **w** systems are shown on the right; the arrow indicates the bond where rupture occurs.

	w-*i*	**w**-*ii*	**w**-*iii*
d(1,2) (Å)	2.65	2.68	2.65
d(2,3) (Å)	2.82	2.85	**2.97**
d(3,4) (Å)	2.64	2.65	2.63
d(4,N_1) (Å)	2.30	2.32	2.28
d(N_2,1) (Å)	**2.53**	**2.48**	2.32
θ_t (°)	31.1	31.4	32.1
F_z^* (nN)	1.40	1.44	1.09
k_z (N/m)	9.25	9.34	7.74
Δz^* (Å)	1.30	1.30	1.30

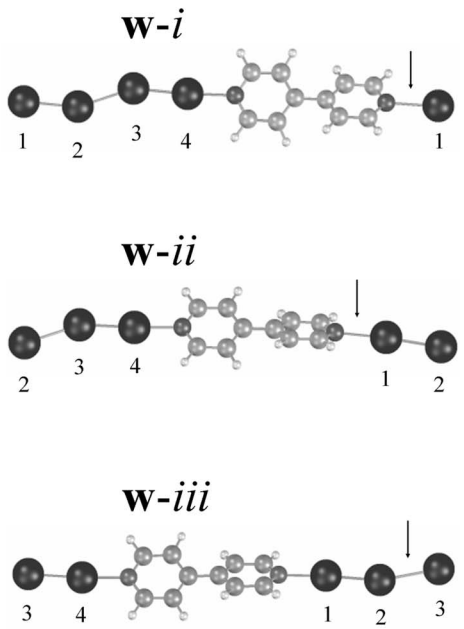

TABLE IV. Relevant bond distances $d(\mathrm{i,j})$ at the rupture configurations of the **w** system of the 1,8 ODT nanojunction. F_z^*, k_z and Δz^* denote the rupture force, force constant and maximum elongation, respectively, and **w**-*i*, **w**-*ii* and **w**-*iii* indicate the rupture procedure according to Fig. 1. The bond distances where rupture occurs are highlighted in bold. The rupture configurations of the three **w** systems are shown on the right; the arrow indicates the bond where rupture occurs.

	w-*i*	**w**-*ii*	**w**-*iii*
d(1,2) (Å)	2.81	**2.94**	2.80
d(2,3) (Å)	**2.92**	2.82	**3.17**
d(3,4) (Å)	2.83	2.79	2.74
d(4,S_1) (Å)	2.39	2.38	2.36
d(S_2,1) (Å)	2.43	2.41	2.38
F_z^* (nN)	1.53	1.78	1.60
k_z (N/m)	6.90	7.90	6.70
Δz^* (Å)	2.40	2.40	2.40

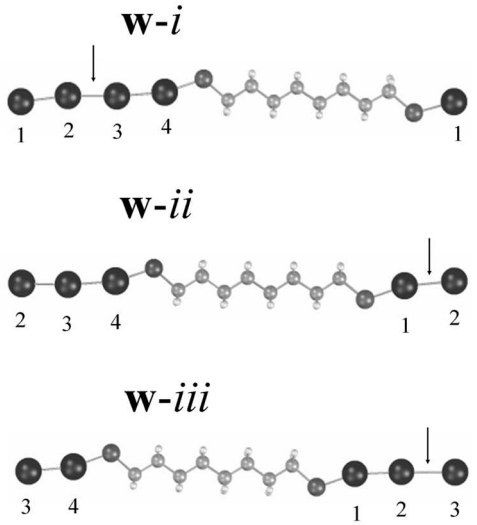

together (1.53–1.60 nN) and similar to the experimental ones (1.5 ± 0.2 nN).[19–22] They were also comparable to previous theoretical values, calculated both for pure Au monatomic nanowires[2,4–9] as for a methanethiol molecule attached to a Au chain.[41,42] As an example, Fig. 3 shows the behavior of the system energy and the force curve in the direction of elongation z for the **w**-*i* system.

It appears that the behavior of 1,8 ODT bound to a Au monatomic chain is similar to that of a pure Au nanowires concerning the maximum (rupture) force F_z^*. The maximum elongation Δz^* found for this nanojunction is 2.40 Å, in good agreement with the value reported for the elongation of a Au chain[18] and somewhat lower than the average value of 3.5 Å found in Ref. 21 for the stretching of 1,8 ODT nanojunction. The force constant calculated here is for the **w**-*i* and **w**-*iii* systems, 6.8 ± 0.2 N/m is in good agreement with the average experimental value of a monatomic Au nanowire

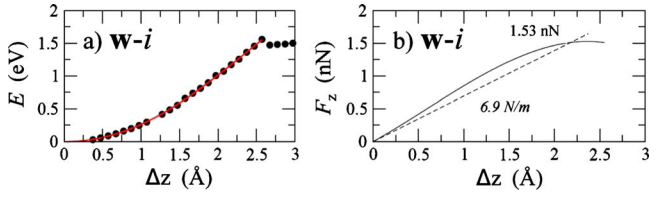

FIG. 3. (Color online) a) System energy E as a function of the elongation Δz for **w**-*i* system of the 1,8 ODT nanojunction. b) z component of the force F_z (solid curve) as a function of elongation Δz and a linear fit of F_z (dashed line) from zero to the maximum force value F_z^* for the **w**-*i*. Values in normal font indicate the maximum rupture force F_z^* and values in italics are the force constants k_z (slopes of the dashed lines) of the different systems.

(8 N/m[2]) and in excellent agreement of the value of 7.2 nN reported for this nanojunction in Ref. 21.

A comparison of Tables III and IV, shows the different nature of both molecular junctions. In particular, from the third column (**w**-*iii* system), we can see that while both systems are broken at the same bond, their mechanical properties are completely different. This means that the properties of the junction depend markedly on the nature of the molecule. The Au-Au bonds distances just before rupture are shorter for 4,4′ BPD than those found for 1,8 ODT. The maximum force is very different, being 1.09 and 1.60 nN for 4,4′ BPD and 1,8 ODT, respectively. The elongation of the junction also marks an important difference between these junctions.

As synthesis for the previous results, we can state that while modeling of the metallic part of the nanojunction as a wire seems to yield reasonable results for 1,8 ODT, this is not the case 4,4′ BPD. The following section is devoted to an improvement of this point.

B. c system

Now, we consider the stretching of molecular nanojunctions for the **c** systems, according to the scheme proposed in Fig. 1. Here, we consider different molecule-Au configurations, starting from a situation where the molecule is directly attached to the metallic electrode (**c**-1 and **c**-2 systems) up to a situation similar to that considered in **w** systems, where the metallic electrode involves chains made of 2, 3 or 4 Au atoms at one end before rupture (**c**-3, **c**-4, and **c**-5 systems).

Table V shows the N-Au bonds distances, the torsion angles and the configurations for the equilibrium geometries

TABLE V. N-Au bond distances d and torsion angles θ_t for the different equilibrium structures of the **c** systems for the 4,4′ BPD nanojunction. The equilibrium structures are shown at the top.

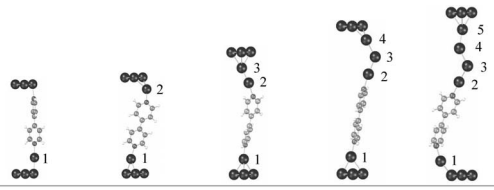

	c-1	**c**-2	**c**-3	**c**-4	**c**-5
$d(1,N_1)$ (Å)	2.22	2.13	2.11	2.14	2.22
$d(N_2,2)$ (Å)	----	2.22	2.15	2.14	2.14
θ_t (°)	34.3	11.5	27.4	23.6	30.7

TABLE VI. S-Au bond distances d for the different equilibrium structures of the **c** systems for the 1,8 ODT nanojunction. The equilibrium structures are shown at the top.

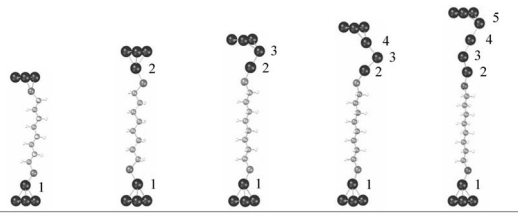

	c-1	**c**-2	**c**-3	**c**-4	**c**-5
$d(1,S_1)$ (Å)	2.32	2.30	2.33	2.31	2.32
$d(S_2,2)$ (Å)	----	2.30	2.32	2.32	2.31

of the different 4,4′ BPD **c** type nanojunctions. It is found that the N-Au equilibrium distances for the **c** systems are between 2.11 and 2.22 Å. The results found for the **w** system are in this same range of values (see Table I), as well as the theoretical values found in Refs. 38 and 52 for this junction. The torsion angle presents a considerable dispersion in their values (11,5–34,3°), with an average value of 25.5°. The latter value is in good agreement with results from first principles calculations performed by Stadler and co-workers.[33] These authors studied the effect of the torsion angle on the conductance and considered the breaking force of a nanojunction built from a molecule of 4,4′ BPD sandwiched between two perfect (111) Au surfaces. They did not found significant change of the results due to the variation of the torsion angle.

Table VI shows the S-Au bonds distances and the configurations for the equilibrium geometries of the 1,8 ODT nanojunction. The S-Au distances practically do not change with the wire length and are equivalent to those determined for the **w** system (see Table II). The equilibrium configurations of the **c**-4 and **c**-5 systems of both (4,4′ BPD and 1,8 ODT) nanojunctions have a monatomic Au chain with a zigzag planar structure, as found in the calculations of monatomic Au nanowires.[55–59]

Figures 4 and 5 shows the behavior of the system energy E and force in the z direction, F_z, as a function of elongation Δz for all **c** systems of the 4,4′ BPD and 1,8 ODT molecular nanojunctions, respectively. The **c**-1, **c**-2, and **c**-3 systems for 4,4′ BPD break at a N-Au bond, specifically **c**-2 and **c**-3 do so at the N_2-Au_2 bond and the **c**-1 system breaks between

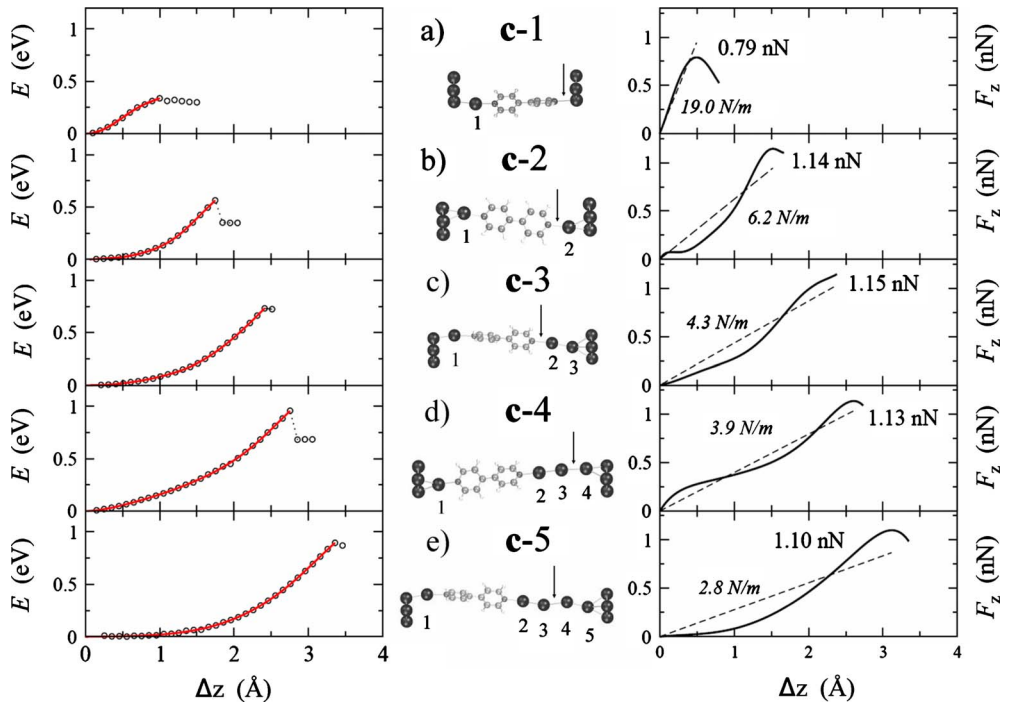

FIG. 4. (Color online) Energies E and the z component of the forces F_z, of the different **c** systems for the 4,4′ BPD nanojunction: a) c-1, b) c-2, c) c-3, d) c-4 e) c-5. The central part of these graphics shows the rupture configurations. Here, the arrow indicates the bond where rupture occurs. In the force graphs the values of rupture force F_z^* are given in normal font and the values of force constant k_z (slope of the dashed line) are given in italics.

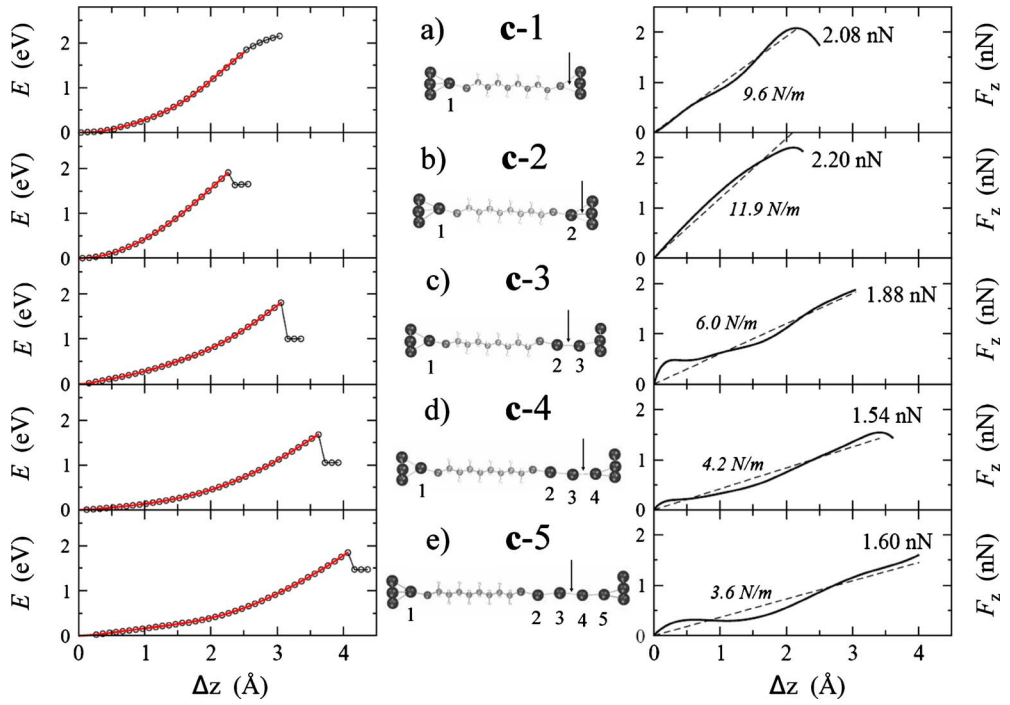

FIG. 5. (Color online) Energies E and the z component of the forces F_z, of the different **c** systems for the 1,8 ODT nanojunction: a) c-1, b) c-2, c) c-3, d) c-4 e) c-5. The central part of these graphics shows the rupture configurations. Here, the arrow indicates the bond where rupture occurs. In the force graphs the values of rupture force F_z^* are given in normal font and the values of force constant k_z (slope of the dashed line) are given in italics.

the N_2 atom and one of the Au atoms forming the triangular base fixed in the process of elongation. The two remaining systems (**c**-4 and **c**-5) break at the Au_2-Au_3 link. Here, is important to note that all values of rupture force are similar and close to 1 nN, regardless of the bond where it occurs.

The theoretical values of rupture forces for the **w** and **c** systems for 4,4′ BPD are closer to the experimental one for two different structural situations in the molecular nanojunction: (*i*) when the 4,4′ BPD molecule is found bound to the electrode through a monatomic chain of 3 or 4 Au atoms, in which case the break would take place on the second link Au-Au (Au_3-Au_4 in the **c** system and Au_2-Au_3 in the **w** system) and (*ii*) when the molecules are attached to a small cluster of Au or when the molecule is linked directly to the electrode surface, in which case the break would take place on the link N-Au.

Ruptures of 1,8 ODT nanojunction occur at some of the Au-Au bonds, except for **c**-1 system, where the Au atoms close the S atom are fixed. The **c**-4 and **c**-5 systems break at the Au_3-Au_4 bond as in the case of 4,4′ BPD. For these system the values of rupture force (1.54 nN for **c**-4 and 1.60 nN for **c**-5) are in excellent agreement with experimental results related to molecular nanojunctions with terminal thiol groups[18–22] or pure Au monatomic chains.[1–3] These results, together with those obtained for the **w** system confirm that 1,8 ODT junctions break at a Au-Au link, after the formation of a monatomic chain of Au as indicated by computer simulations.[41,42]

An estimation of the energies of the broken bonds for the different nanojunctions can be obtained from the energy curves of Figs. 4 and 5. The **c**-4 and **c**-5 systems break at the same bond (Au_3-Au_4), irrespective of the molecule involved in the molecular nanojunction. However, the energy of this bond is about 1 eV for 4,4′ BPD and 2 eV for 1,8 ODT nanojunctions. The 1,8 ODT **c**-1 system, as already mentioned, breaks at the S-Au bond and its energy at rupture elongation is greater than 2 eV. The value of the energies of the N-Au bond, depending on the system (**c**-1, **c**-2, or **c**-3) for 4,4′ BPD varies between 0.4 and 0.7 eV. This estimate agrees with previously reported results for the cohesive energy of a pyrazine molecule attached to a cluster of 6 atoms of Au.[43]

Figure 6 summarizes results obtained from the mechanical stretching for the most relevant **c** systems for both nanojunctions. This graph compares the results obtained here with the experimental values of Ref. 21. The x axis represents the number of Au atoms involved in molecular junction, where the **c**-1 system contributes with 1, **c**-2 with 2, **c**-3 with 3, **c**-4 with 4 and **c**-5 with 5 Au atoms. From these results we conclude that the configuration of the 1,8 ODT nanojunction most likely found in the experiments, according to our model calculations should correspond to the **c**-4 and **c**-5 systems. In particular, the agreement with the experimental values of F_z^*, k_z, and Δz^* with our calculations is very good for the **c**-4 system. In the case of the 4,4′ BPD nanojunction, the Fig. 6 shows that the configuration that best correlates with the experiments would be one where the molecule is connected to the electrode through a chain of 3 or 4 atoms Au. The **c**-4 and **c**-5 system fit very well with the experimental values of F_z^*, k_z, and Δz^*. Nevertheless it is clear that our model calculation is only approximate. On the one hand, the model with a small number of atoms is not faithful representation of

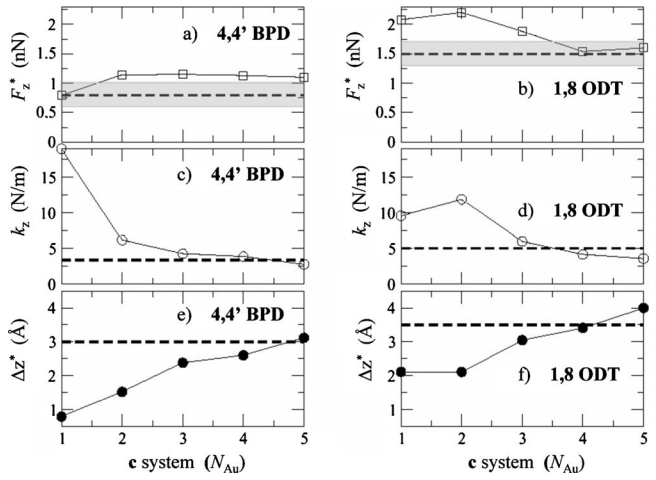

FIG. 6. a) and b) rupture force F_z^*, c) and d) force constant k_z, e) and f) maximum elongation Δz^* for the 4,4′ BPD and 1,8 ODT molecular nanojunctions, respectively. The x-axis represents the number of Au atoms in the chain of the different **c** systems. The dashed horizontal lines indicate the experimental values of F_z^*, k_z, and Δz^* extracted from Ref. 21. The gray area in a) and b) represents the region defined by the experimental error bars.

the metal electrode and the other, the settings chosen to begin the process of stretching are arbitrary. In this respect, the calculation model does not take into account the insertion mechanism of molecules between electrodes.

The results discussed above suggest that both nanojunctions are linked to a monatomic chain of 3 or 4 atoms of Au before breaking. According to the results presented here, both nanojunctions break on the same bond (Au_3-Au_4) but with different values of rupture force. This may due in principle to the fact that the molecule affects and modifies the chemical environment of the system, particularly the type of bonding between the Au atoms forming the monatomic chain. For this reason, this effect will be analyzed in the following discussion correlating structure, energy, and electronic nature of the most relevant N-Au, S-Au, Au-Au bonds of the **c**-4 and **c**-5 system. This will be done for both molecular nanojunctions at their equilibrium ($\Delta z=0$) and maximum force ($\Delta z=\Delta z^*$) elongations. A useful tool to analyze the thermodynamic stability of a bond of the system, is the vertical fragmentation energy E_{A-B}^{frag}. For a A-B system, according to Ref. 60 this energy is defined as:

$$E_{A-B}^{\text{frag}} = E_A + E_B - E_{A-B}, \tag{1}$$

where E_{A-B} is the energy of the A-B system and E_A and E_B are the energies of the A and B subsystems, respectively. Our simulation model is infinite in the z-axis direction, so the vertical fragmentation energy in this case relates to the energy of the system fragmented at the bond of interest (the fragments are separated elongating the unit cell along the z axis to a distance where they do not interact), minus the energy of the unfragmented system. Table VII shows the bond order q (calculated according to the Mulliken overlap

TABLE VII. Bond order q, vertical fragmentation energy E_{A-B}^{frag} and bond distance d for the most relevant bonds of the 4,4′ BPD and 1,8 ODT nanojunctions of the **c**-4 system. In each case we considered the equilibrium (Δz_e) and rupture (Δz^*) configurations.

c-4 **c-4**

Δz_e

	N_2-Au_2	Au_2-Au_3	Au_3-Au_4	S_2-Au_2	Au_2-Au_3	Au_3-Au_4
q (a.u.)	0.192	0.260	0.136	0.292	0.190	0.182
E^{frag} (eV)	1.17	2.42	0.84	2.34	1.35	1.29
d (Å)	2.14	2.58	2.70	2.32	2.64	2.65

Δz^*

	N_2-Au_2	Au_2-Au_3	Au_3-Au_4	S_2-Au_2	Au_2-Au_3	Au_3-Au_4
q (a.u)	0.104	0.268	0.119	0.257	0.169	0.168
E^{frag} (eV)	0.76	2.19	0.60	1.81	0.88	0.91
d (Å)	2.39	2.68	2.99	2.42	2.91	2.95

TABLE VIII. Bond order q, vertical fragmentation energy E_{A-B}^{frag} and bond distance d for the most relevant links of the 4,4′ BPD and 1,8 ODT nanojunctions of the **c**-5 system. In each case we considered the equilibrium (Δz_e) and rupture (Δz^*) configurations.

c-5 **c-5**

Δz_e

	N_2-Au_2	Au_2-Au_3	Au_3-Au_4	Au_4-Au_5	S_2-Au_2	Au_2-Au_3	Au_3-Au_4	Au_4-Au_5
q (a.u.)	0.169	0.275	0.144	0.279	0.294	0.183	0.224	0.162
E^{frag} (eV)	1.05	2.72	0.84	2.14	2.60	1.16	1.80	1.04
d (Å)	2.14	2.56	2.66	2.58	2.31	2.65	2.63	2.68

Δz^*

	N_2-Au_2	Au_2-Au_3	Au_3-Au_4	Au_4-Au_5	S_2-Au_2	Au_2-Au_3	Au_3-Au_4	Au_4-Au_5
q (a.u.)	0.114	0.273	0.117	0.256	0.263	0.171	0.162	0.209
E^{frag} (eV)	0.65	2.43	0.60	1.90	2.03	0.91	0.94	1.25
d (Å)	2.33	2.66	2.94	2.69	2.40	2.88	2.99	2.81

population),[61] the vertical fragmentation energy E_{A-B}^{frag} and bond distance d for the most relevant N-Au, S-Au, Au-Au bonds of both nanojunctions for the **c**-4 system. Overall, we can see that in both nanojunctions, the transition from the equilibrium configuration Δz_e to the rupture configuration Δz^* causes an elongation of both, the Au_2-Au_3 and Au_3-Au_4 bonds, the later to a greater extent. This is accompanied by a decrease in E_{A-B}^{frag} as expected. On the other hand, the correlation with q is not clearcut, since in the case of 4,4′ BPD q shows a small increase. The differences in the rupture forces can then be understood comparing the columns of Au_3-Au_4 bonds between the two nanojunctions. For this link and at the rupture elongation Δz^*, E_{A-B}^{frag} are 0.60 and 0.91 eV for 4,4′ BPD and 1,8 ODT, respectively. The bond order of the Au_3-Au_4 bond follows the same trend for both elongations (Δz_e, Δz^*). Thus, the larger value of bond order and fragmentation energy for the Au_3-Au_4 bond of the 1,8 ODT system suggests that this link is stronger and thermodynamically more stable than the Au_3-Au_4 bond of the 4,4′ BPD nanojunction. This also explains the larger rupture force of 1,8 ODT with respect to 4,4′ BPD, when both links are broken at the same Au_3-Au_4 bond.

Table VIII shows the values of q, E_{A-B}^{frag} and d for the **c**-5 system involving both link molecules at their equilibrium and rupture elongations. The conclusions drawn from the analysis of this table are in principle equivalent to those extracted from Table VII. The Au-Au distances at the rupture configurations of both nanojunctions indicate the formation of Au dimers, just as it happens in the case of pure Au monatomic chains.[55–59] This phenomenon, known as Peierls dimerization is evident in these systems and appears as particularly important for 4,4′ BPD nanojunction. This nanojunction exhibits at the rupture elongation alternating short Au-Au bond distances (~2.66 Å) with longer ones (2.94 Å). This feature, combined with the high vertical fragmentation energy of the Au_2-Au_3 (2.43 eV) and Au_4-Au_5 (1.90 eV) bonds, suggests the existence of conjugation in the bonds of the monatomic Au chain for the 4,4′ BPD nanojunction. Similar results in terms of bond distances, vertical fragmentation energies and bond order have been reported by our research group[43] for the mechanical stretching of a pyrazine molecule attached to a small Au cluster via a planar monatomic chain of 3, 4, or 5 Au atoms.

Based on the q and E_{A-B}^{frag} values, we have shaded gray in Tables VII and VIII those columns corresponding to the two bonds with the larger rupture probability. Considering the configuration of maximum force (Δz^*), we find that the weaker bonds in both **c**-4 and the **c**-5 systems are the same for both link molecules. Focusing on the E_{A-B}^{frag} and q values for the Δz^* configuration of the **c**-4 system (Table VII), we see that the 4,4′ BPD nanojunction could break at the N_2-Au_2 bond (0.76 eV–0.10 a.u.) and also at the Au_3-Au_4 bond (0.60 eV–0.12 a.u.), while the 1,8 ODT nanojunction could break at the Au_2-Au_3 (0.88 eV–0.17 a.u.) bond and also at the Au_3-Au_4 bond (0.91 eV–0.17 a.u.). Using the present stretching procedure, we find that both nanojunctions break actually at the Au_3-Au_4 bond in the **c**-4 and **c**-5 systems. However, the vertical fragmentation energies of the N_2-Au_2 and Au_3-Au_4 links for 4,4′ BPD are very similar, and something similar happens with the Au_2-Au_3 and Au_3-Au_4 bonds for 1,8 ODT. Even more, the single consideration of the vertical fragmentation energy for the latter system would suggest that the 1,8 ODT junction should rather break at the Au_2-Au_3, something that is not really observed. This contradiction, although not severe due to the small energy differences, lead us to go more into the details of the rupture process from a kinetic viewpoint.

In chemistry, kinetic processes are often analyzed in the framework of transition state theory,[62,63] where the saddle

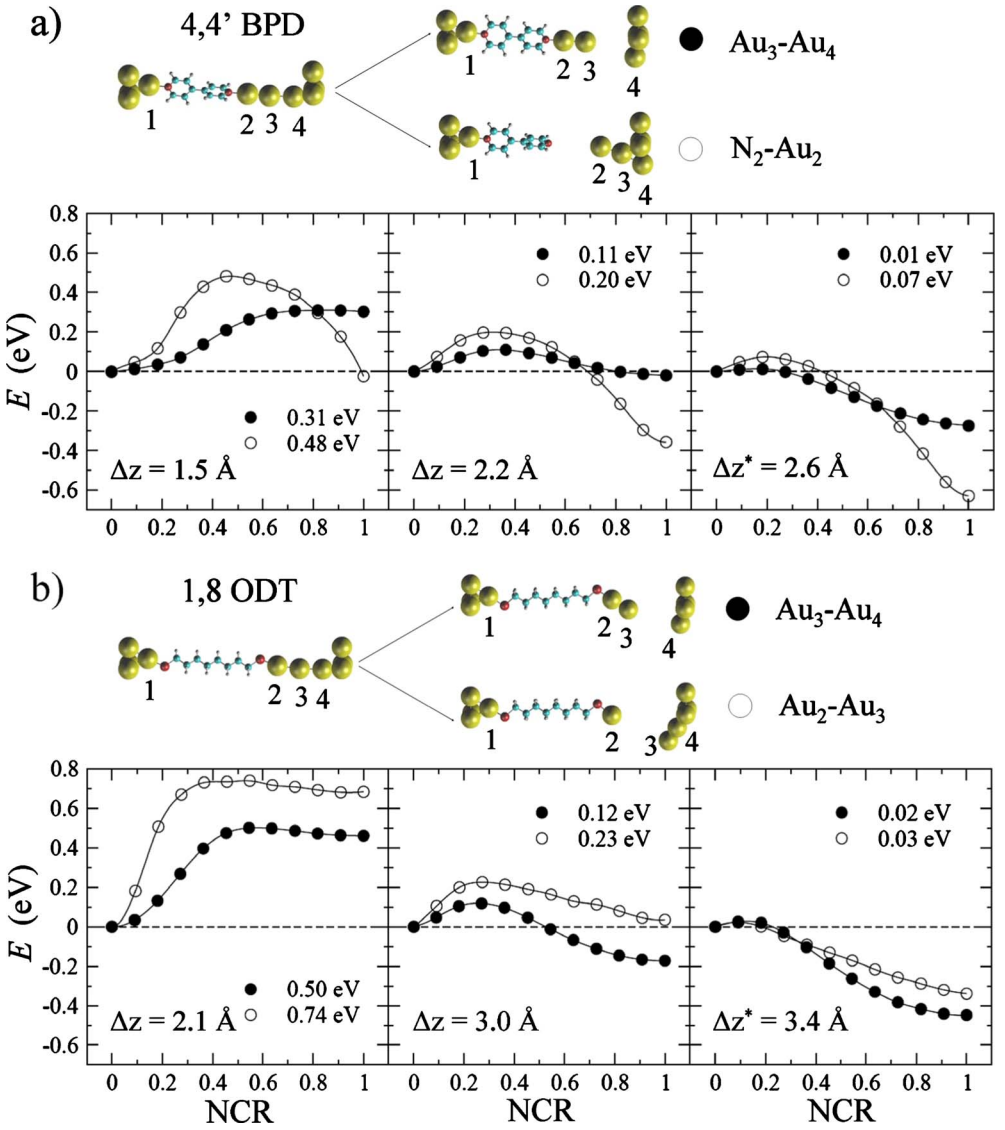

FIG. 7. (Color online) Energy E as function of the normalized reaction coordinate (NRC) of the **c**-4 system for different elongations Δz close to the rupture configuration. a) 4,4′ BPD: (●) MEP for rupture at the Au_3-Au_4 bond, (○) MEP for rupture at the N_2-Au_2 bond. b) 1,8 ODT: (●)MEP for rupture at the Au_3-Au_4 bond, (○)MEP for rupture at the Au_2-Au_3 bond.

point found between reactants and products in the Born-Oppenheimer surface plays a key role. There, the energy difference found between that of the system at the saddle point and the energy of the reactants is denominated activation energy, and represents the energetic barrier that the system must surmount to undergo the reaction. We have found these concept useful to analyze the stability of pure Au nanowires,[8] as well as contaminated with atomic impurities,[9] and we use in the following the same ideas to analyze the kinetic stabilities of the present system. Considering the system for a given elongation (Δz), we take as the initial state (reactants) that of the unbroken wire, and as final state (products) that of the broken wire. We performed calculations for the **c**-4 system for both nanojunctions. The wire was broken at the bond of interest, and the energy of the system was minimized using the conjugate gradient technique. This defined the configuration of the final state. The procedure used to obtain the minimum energy path between reactants and products was described in Sec. II and from it the activation energy for the different processes was obtained.

Figure 7 shows the energy profiles versus the normalized reaction coordinate (NRC) for three elongations Δz close to the rupture of such systems. We considered ruptures at the N_2-Au_2 and Au_3-Au_4 bonds for 4,4′ BPD [Fig. 7(a)] and rupture at the Au_2-Au_3 and Au_3-Au_4 bonds for 1,8 ODT [Fig. 7(b)]. Figure 7 also shows the geometric configurations for the fragmented and unbroken states of both nanojunctions. The former showed almost no changes for the different elongations considered.

Figure 7(a) shows that the activation energies near the limit of mechanical stability of the 4,4′ BPD nanojunction are always higher to break the system at the N_2-Au_2 bond than to break it at the Au_3-Au_4 bond. This is consistent with the rupture found at the Au_3-Au_4 bond encountered during the mechanical stretching process. However, for smaller elongations, rupture at the Au_3-Au_4 delivers a status of the

system that is energetically unstable, in the sense that a backward reaction is unactivated. In the case of the 1,8 ODT nanojunction, Fig. 7(b) shows that from a kinetic viewpoint, the Au_3-Au_4 bond of 1,8 ODT nanojunction should break more easily than Au_2-Au_3 bond than at the Au_2-Au_3 bond, also in agreement with the results of mechanical stretching. Based on the above, we were able to corroborate from a kinetic point of view that the Au_3-Au_4 bond of the **c**-4 system for both nanojunctions is broken most likely.

IV. CONCLUSIONS

In this work we have focused our attention on the comparative study of the mechanical properties of 4,4′ BPD and 1,8 ODT molecular nanojunctions. Using two different model calculation involving metal wires and small clusters for these nanojunctions, a mechanical stretching procedure was used to monitor the rupture of the systems at some of their links.

The information extracted from the mechanical stretching process in all cases was compared with the experimental values of rupture force, constant force, and distance of maximum elongation before rupture. The results obtained for the mechanical stretching of the 1,8 ODT junction for the **w** and **c** systems, are in good agreement with experimental results. We found that the rupture at Au-Au bonds is energetically favored over rupture at the S-Au bond. In particular, the **c**-4 system fits very well with the experimental results of Ref. 21. For this system the measured values of F_z^*, k_z, and Δz^* were 1.54 nN, 4.2 N/m and 3.41 Å, respectively. Moreover the mechanical behavior of this molecular nanojunction is very similar to that of a pure Au monatomic nanowire.

The 4,4′ BPD molecular nanojunction presents a less clearcut behavior than that of 1,8 ODT behavior. Summarizing the results of the two considered systems, wires and clusters, we distinguish two different mechanical situations for this nanojunction. When the molecule is bound to a small gold cluster, the present calculations predict that this junction should break at the N-Au bond with rupture force of 0.79 nN (**c**-1 system), 1.14 nN (**c**-2 system) and 1.15 nN (**c**-3 system). However, when 4,4′ BPD is stretched attached to a chain of Au atoms, the prediction is that rupture should occur at the second Au-Au bond of this chain. The rupture force results of the **w** and **c** systems are similar: 1.09 nN (**w**-*iii* system), 1.13 nN (**c**-4 system) and 1.10 nN (**c**-5 system). Comparison of the calculated force constants and stretching lengths with experimental values of Ref. 21 suggest that the most usual configuration of the 4,4′ BPD molecular nanojunction in the experiments, should correspond to the molecule of 4,4′-bipyridine attached to massive metal to a chain of Au monatomic 3 or 4 atoms at one end.

ACKNOWLEDGMENTS

Financial support from CONICET, Secyt UNC, and Program BID 1728/OC-AR PICT No. 946 are gratefully acknowledged. P.V. thanks CONICET.

*Corresponding author; eze_leiva@yahoo.com.ar

[1] G. Rubio, N. Agraït, and S. Vieira, Phys. Rev. Lett. **76**, 2302 (1996).
[2] G. Rubio-Bollinger, S. R. Bahn, N. Agraït, K. W. Jacobsen, and S. Vieira, Phys. Rev. Lett. **87**, 026101 (2001).
[3] T. Kizuka, Phys. Rev. B **77**, 155401 (2008).
[4] E. Z. da Silva, F. D. Novaes, A. J. R. da Silva, and A. Fazzio, Phys. Rev. B **69**, 115411 (2004).
[5] A. Nakamura, M. Brandbyge, L. B. Hansen, and K. W. Jacobsen, Phys. Rev. Lett. **82**, 1538 (1999).
[6] F. D. Novaes, A. J. R. da Silva, E. Z. da Silva, and A. Fazzio, Phys. Rev. Lett. **90**, 036101 (2003).
[7] P. Vélez, S. A. Dassie, and E. P. M. Leiva, Phys. Rev. Lett. **95**, 045503 (2005).
[8] P. Vélez, S. A. Dassie, and E. P. M. Leiva, Chem. Phys. Lett. **460**, 261 (2008).
[9] P. Vélez, S. A. Dassie, and E. P. M. Leiva, Phys. Rev. B **81**, 125440 (2010).
[10] H. Ohnishi, Y. Kondo, and K. Takayanagi, Nature (London) **395**, 780 (1998).
[11] A. I. Yanson, G. Rubio Bollinger, H. E. van den Brom, N. Agrait, and J. M. van Ruitenbeek, Nature (London) **395**, 783 (1998).
[12] J. I. Pascual, J. Méndez, J. Gómez-Herrero, A. M. Baró, N. García, and V. T. Binh, Phys. Rev. Lett. **71**, 1852 (1993).
[13] Q. Pu, Y. Leng, H. S. Park, S. T. Pantelides, and P. T. Cummings, J. Chem. Phys. **126**, 144707 (2007).
[14] T. N. Todorov and A. P. Sutton, Phys. Rev. Lett. **70**, 2138 (1993).
[15] S. R. Bahn and K. W. Jacobsen, Phys. Rev. Lett. **87**, 266101 (2001).
[16] W. Haiss, R. J. Nichols, H. V. Zallinge, S. J. Higgins, D. Bethell, and D. J. Schiffrin, Phys. Chem. Chem. Phys. **6**, 4330 (2004).
[17] W. Haiss, C. Wang, I. Grace, A. S. Batsanov, D. J. Schiffrin, S. J. Higgins, M. R. Bryce, C. J. Lambert, and R. J. Nichols, Nature Mater. **5**, 995 (2006).
[18] Z. Huang, F. Chen, P. A. Bennett, and N. J. Tao, J. Am. Chem. Soc. **129**, 13225 (2007).
[19] Z. Huang, B. Xu, Y. Chen, M. Di Ventra, and N. J. Tao, Nano Lett. **6**, 1240 (2006).
[20] X. Li, J. He, B. Xu, S. M. Lindsay, and N. J. Tao, J. Am. Chem. Soc. **128**, 2135 (2006).
[21] B. Xu, X. Xiao, and N. J. Tao, J. Am. Chem. Soc. **125**, 16164 (2003).
[22] B. Q. Xu, X. L. Li, X. Y. Xiao, H. Sakaguchi, and N. J. Tao, Nano Lett. **5**, 1491 (2005).
[23] B. Xu and N. J. Tao, Science **301**, 1221 (2003).
[24] Z. Huang, F. Chen, R. D'Agosta, P. A. Benett, M. Di Ventra, and N. J. Tao, Nat. Nanotechnol. **2**, 698 (2007).
[25] C. Li, I. Pobelov, T. Wandlowski, A. Bagrets, A. Arnold, and F. Evers, J. Am. Chem. Soc. **130**, 318 (2008).
[26] X. D. Cui, A. Primak, X. Zarate, J. Tomfohr, O. F. Sankey, A. L. Moore, T. A. Moore, D. Gust, G. Harris, and S. M. Lindsay,

Science **294**, 571 (2001).
[27] M. S. Hybertsen, L. Venkataraman, J. E. Klare, A. C. Whalley, M. L. Steigerwald and C. Nuckolls, J. Phys.: Condens. Matter **20**, 374115 (2008).
[28] L. Venkataraman, Y. S. Park, A. C. Whalley, C. Nuckolls, M. S. Hybertsen, and M. L. Steigerwal, Nano Lett. **7**, 502 (2007).
[29] Y. S. Park, A. C. Whalley, M. Kamenetska, M. L. Steigerwald, M. S. Hybertsen, C. Nuckolls, and L. Venkataraman, J. Am. Chem. Soc. **129**, 15768 (2007).
[30] R. J. C. Batista, P. Ordejón, H. Chacham, and E. Artacho, Phys. Rev. B **75**, 041402 (2007) R.
[31] M. Paulsson, C. Krag, T. Frederiksen, and M. Brandbyge, Nano Lett. **9**, 117 (2009).
[32] Y. H. Kim, J. Tahir-Kheli, P. A. Schultz, and W. A. Goddard III, Phys. Rev. B **73**, 235419 (2006).
[33] R. Stadler, K. S. Thygesen, and K. W. Jacobsen, Phys. Rev. B **72**, 241401(R) (2005).
[34] Z. L. Li, B. Zou, C. K. Wang, and Y. Lou, J. Phys.: Conf. Ser. **29**, 110 (2006).
[35] Z. L. Li, B. Zou, C. K. Wang, and Y. Luo, Phys. Rev. B **73**, 075326 (2006).
[36] X. Wu, Q. Li, J. Huang, J. Yang, and J. Chem, Physica **123**, 184712 (2005).
[37] Q. Li, X. Wu, J. Huang, and J. Yang, Ultramicroscopy **105**, 293 (2005).
[38] S. Hou, J. Zhang, R. Li, J. Ning, R. Han, Z. Shen, X. Zhao, Z. Xue, and Q. Wu, Nanotechnology **16**, 239 (2005).
[39] A. Pérez-Jiménez, J. Phys. Chem. B **109**, 10052 (2005).
[40] P. Vélez, S. A. Dassie, and E. P. M. Leiva, in *Recent Advances in Nanoscience*, edited by M. M. Mariscal and S. A. Dassie (Research Signpost, Kerala, India, 2007), Chap. 1, p. 1.
[41] D. Krüger, R. Rousseau, H. Fuchs, and D. Marx, Angew. Chem., Int. Ed. **42**, 2251 (2003).
[42] D. Krüger, H. Fuchs, R. Rousseau, D. Marx, and M. Parrinello, Phys. Rev. Lett. **89**, 186402 (2002).
[43] M. F. Zoloff Michoff, P. Vélez, and E. P. M. Leiva, J. Chem. Phys. C **113**, 3850 (2009).
[44] M. E. Zoloff Michoff, P. Vélez, S. A. Dassie, and E. P. M. Leiva, in *Electrodeposited Nanowires and their Applications*, edited by Nicoleta Lupu (InTech, Vukovar, Croacia, 2010), Chap. 1.
[45] P. Ordejón, E. Artacho, and J. M. Soler, Phys. Rev. B **53**, R10441 (1996).
[46] D. Sáchez-Portal, P. Ordejón, and E. Artacho, Int. J. Quantum Chem. **65**, 453 (1997).
[47] E. Artacho, D. Sánchez-Portal, P. Ordejón, A. García, and J. M. Soler, Phys. Status Solidi **215**, 809 (1999) b.
[48] P. Ordejón, D. Sánchez-Portal, A. García, E. Artacho, J. Junquera, and J. M. Soler, RIKEN Rev. **29**, 42 (2000).
[49] J. M. Soler, E. Artacho, J. D. Gale, A. García, J. Junquera, P. Ordejón, and D. Sánchez-Portal, J. Phys.: Condens. Matter **14**, 2745 (2002).
[50] S. A. Trygubenko and D. Wales, J. Chem. Phys. **120**, 2082 (2004).
[51] D. C. Liu and J. Nocedal, Math. Program. **45**, 503 (1989).
[52] S. Hou, J. Ning, Z. Shen, X. Zhao, and Z. Xue, Chem. Phys. **327**, 1 (2006).
[53] A. Almenningen, O. Bastiansen, and K. Nor. Vidensk, Selsk. Skr. **4**, 1 (1958).
[54] F. P. Cometto, P. Paredes-Olivera, V. A. Macagno, and E. M. Patrito, J. Phys. Chem. B **109**, 21737 (2005).
[55] M. Okamoto and K. Takayanagi, Phys. Rev. B **60**, 7808 (1999).
[56] J. Nakamura, N. Kobayashi, and M. Aono, RIKEN Rev. **37**, 17 (2001).
[57] D. Sánchez-Portal, E. Artacho, J. Junquera, P. Ordejón, A. García, and J. M. Soler, Phys. Rev. Lett. **83**, 3884 (1999).
[58] S. R. Bahn, N. López, J. K. Nørskov, and K. W. Jacobsen, Phys. Rev. B **66**, 081405 (2002) R.
[59] L. De Maria and M. Springborg, Chem. Phys. Lett. **323**, 293 (2000).
[60] M. Konopka, R. Turansky, J. Reichert, H. Fuchs, D. Marx, and I. Stich, Phys. Rev. Lett. **100**, 115503 (2008).
[61] A. Szabo and N. Ostlund, *Modern Quantum Chemistry* (McGraw-Hill, New York, 1989).
[62] H. Eyring, J. Chem. Phys. **3**, 107 (1935).
[63] G. H. Vineyard, J. Phys. Chem. Solids **3**, 121 (1957).